University of Iowa 68-1

Absolute Optical Flux Observations of the 18 October 1967 Total Eclipse of the Moon

by

J.S. Neff

Department of Physics and Astronomy
University of Iowa
Iowa City, Iowa

January 1968

* This research was supported in part by the National Aeronautics and Space Administration under Grant NsG 233-62.

ABSTRACT

Absolute optical flux observations at $\lambda = 0.33\ \mu$, $0.37\ \mu$, $0.47\ \mu$ and $0.55\ \mu$ are presented for the descending branch and total phase of the 18 October 1967 lunar eclipse. A brief description of the photometer and photometric system is given with a discussion of the observational and reduction procedures for the lunar photometry.

The observed photon flux at the top of the earth's atmosphere is converted into the photon flux incident on the moon and the ratio of this flux to that of the uneclipsed sun (attenuation factor) is calculated. The eclipse was a normal eclipse, the attenuation factor at $\lambda = 0.55\ \mu$ was 10^{-5} and the moon was red, i.e. $B - V \tilde{=} 6$. The attenuation versus time curves were asymmetrical for the longer wavelengths.

The integrated energy flux for the $0.33 - 0.55\ \mu$ spectral region was compared with the charged particle energy flux on the lunar surface, for the purpose of examining the possibility of direct excitation of lunar luminescence. The charged particle fluxes were determined from observations by Explorer 35, orbiting the moon, and OGO III and Explorer 34 inside the magnetosphere. Only two sources of irradiation of the lunar surface were comparable

in magnitude to the integrated optical flux. These were low energy protons and electrons and the UV spectrum of the outer solar corona. The sources are estimated to produce an intensity of luminescent photons that is a percent or less of the observed flux of optical photons.

1. Introduction

Observations of the total eclipse of the moon by the earth on 18 October 1967 were made with the integrating digital photometer on the 24 inch (61cm) Cassegrain reflecting telescope of the University of Iowa Observatory for the purpose of obtaining light curves for wavelength regions centered at 0.34 μ, 0.37 μ, 0.47 μ, and 0.55 μ. Such observations can yield information on the relative importance of extinction in the terrestrial atmosphere due to dust or clouds. Analysis of such observations can provide a determination of the altitude and total extinction of the dust layer and an approximate value for the amount of ozone in the atmosphere along the terminator of the earth. This analysis is delayed pending assembly of necessary data.

Observations of an eclipse of the sun by the earth were made simultaneously in the 2-12Å region of the x-ray spectrum with the University of Iowa detector GM1 on the lunar orbiting satellite Explorer 35 [Van Allen, 1967]. These data provide information on the x-ray opacity of the earth's upper atmosphere.

This is the first lunar eclipse since Explorer 35 was placed in orbit about the moon presenting a unique opportunity to compare the directly measured energy flux due to particles on the moon's surface to the observed optical flux from the totally eclipsed moon.

2. Observations

A photometric system employing interference filters was used in this study. A detailed description of this system and the data reduction procedures has been given by Neff and Travis [1967]. The photometer employed is very similar to the one used at the McDonald Observatory and was constructed at the University of Iowa under the direction of J.S. Neff. The electronics used in this study differ from those described above and a block diagram of the system is shown in Figure 1. A detailed description of this system is available [Neff, Carlson and Becker, 1967].

Extensive lists of photometric measurements of standard stars are given by Neff and Travis [1967] and Neff [1967]. The photometric data are given in magnitudes normalized to a mean star of spectral type AOV and in monochromatic fluxes in cgs units. For this study the flux in photons $(cm^2\ sec)^{-1}$ at the top of the earth's atmosphere is a more appropriate unit and the relations between photon flux and the four magnitude scales are given in Table I with other relevant characteristics of the photometric system.

Standard stars observed near the end of the night had significant departures from their mean values which showed that the transparency of the sky was becoming variable. This is unfortunate

because the moon was observed at a large air mass at this time and an uncertainty in transparency introduces a systematic error in the observed flux.

3. Observational and Reduction Procedures for Lunar Photometry

A relatively smooth region of the moon at -35° selenographic longitude and +23° selenographic latitude was observed with diaphragms of 1 and 2mm diameter giving projected angular diameters of 20" and 40" respectively. The change from the 1 to 2mm diaphragm occurred at 9.2 UT. The uneclipsed moon was too bright to observe and attenuating screens available at the time did not have sufficient range. We were reluctant to reduce the photomultiplier voltage because of the possibility of introducing non linear and therefore poorly determined transformations between lunar and stellar observations.

Some difficulty in obtaining accurate centering on the moon was encountered during the early partial phases of the eclipse. The high contrast between the uneclipsed and eclipsed portions of the moon made it difficult to see features on the eclipsed portion. After the first three observations, no further difficulty was encountered in centering. A sky reading was taken approximately 3' from the east limb of the moon, after each observation of the moon.

The total number of pulses recorded by the digital integrator was normalized to: pulses/sec, the highest amplifier gain and to the 2mm diaphragm. This was checked against the parallel output on the strip chart recorder and the internal consistency was very good.

Sky corrections were determined by interpolating in a semi log plot of sky reading versus UT. Sky corrections are a source of uncertainty in these observations because of their rapid variations with time and position near the moon.

The observations of the moon, corrected for sky, were corrected for atmospheric extinction. The air mass varied from 1.5 to 3.2. The intensity above the atmosphere (in pulses/sec) was converted into a photon flux [photons $(cm^2 sec)^{-1}$] using conversion factors determined from observations of standard stars.

4. Determination of the Photon Flux Incident on the Moon's Surface

In the previous section, the photon flux from the moon observed at the top of the atmosphere was obtained. The desired quantity for comparison with theory is the monochromatic attenuation factor (A_σ) or the ratio of the photon flux incident on the moon to the flux from the uneclipsed sun. The photon flux from the sun for each wavelength is given in Table I. The calculation

of the photon flux incident on the moon is given in Table II. The observed flux at the top of the earth's atmosphere, the calculated flux incident on the moon and A_σ are given in Table III as functions of UT. The A_σ's are plotted against Universal Time in Figure 2.

The tabulated errors of the observed flux are estimated mean errors and include the uncertainty in the sky correction. The estimated error in the photon flux from the uneclipsed sun is 10% based on the agreement with a number of other determinations [Neff, 1967]. The geometric albedos are probably uncertain by 5%. Thus A_σ is estimated to be uncertain by 15-25%.

5. Systematic Errors

The systematic errors in the flux calibration and in the determination of the solar flux at 1 A.U. have been discussed previously [Neff, 1967].

As was mentioned in an earlier section, observations of the moon, after totality, may be systematically in error by 10-15% due to a suspected change in transparency of the atmosphere.

The systematic errors introduced by the use of a calculated flux from the uneclipsed moon are: the error in the absolute flux from the sun, the use of a mean geometric albedo, interpolated from values given by Harris [1961], rather than the albedo of the observed point of the moon.

On the other hand the use of a measured flux at some later full moon will not appreciably improve the accuracy, because the correction for the difference in phase factor is uncertain. The phase factor during eclipse was very close to 1 as the phase angle varied between 15'- 40'.

6. Discussion

The variations in A_σ and regular distance from the umbra center with UT are shown in Figures 2a and 2b. The attenuation curves show a marked asymmetry when plotted versus angular distance from the umbra center. This asymmetry is much larger than can be attributed to a systematic error due to a change in transparency of the sky. The asymmetry is apparently due to the nonuniform illumination of the moon during total eclipse, which was noticed by visual observers all over the United States and is apparent on photographs [Sky and Telescope, December 1967]. The nonuniform illumination of the moon could be due to a variable distribution of clouds along the terminator of the earth.

To predict theoretical attenuation curves for this eclipse a knowledge of the distribution and altitudes of clouds along the earth's terminator is necessary. In addition empirical data on the attenuation and refraction of light by clouds are required. At the

present time only white light data are available and they may not be sufficient.

Information on cloud distribution and altitudes is being assembled from synoptic maps, where available, and satellite photographs. In this study the attenuation by high altitude clouds composed of ice crystals is likely to be most important, and these clouds can easily be recognized on satellite photographs.

7. Direct Excitation of Lunar Luminiscence

The simultaneous measurement of the incident charged particle and solar wind flux near the moon, and the optical flux from the totally eclipsed moon presents a unique opportunity to examine the possibility of direct excitation of lunar luminescence. Ney, Woolf and Collins [1965] have discussed this problem and we apply their method of analysis to the 18 October 1967 eclipse.

The sources of irradiation of the lunar surface are: electrons and protons, hot plasma inside the magnetosphere, soft UV from the outer corona and cosmic rays. The measured or limiting values for the proton, electron, and plasma fluxes on the moon measured by Explorer 35 for the 18 October 1967 eclipse were kindly provided by J.A. Van Allen, S.M. Krimigis, of the University of

Iowa, and A. Lazarus of M.I.T. prior to publication. The effective cosmic ray flux is the fraction of the cosmic ray energy flux, $\sim 10^{-3}$ erg$(cm^2 sec)^{-1}$, dissipated within one optical depth of the moon's surface.

The values for the energy flux on the lunar surface due to low energy electrons and protons are required. These quantities were not measured on Explorer 35 and the plasma probe was below its threshold. L.A. Frank [1967] has low energy proton and electron detectors on the earth orbiting satellites OGO III and Explorer 34, and he has provided representative values for the energy density and mean energy for protons and electrons inside the magnetosphere at distance ranging from $20R_E$ to $35R_E$ for OGO III and Explorer 34 respectively. The values are $< 5 \times 10^{-11}$ erg cm^{-3} to 2×10^{-9} erg cm^{-3} and $\bar{E}_p = 1$ - 10 kev for protons and 10^{-11} erg cm^{-3} to 5×10^{-9} erg cm^{-3} and $\bar{E}_e = 0.2$ - 3 kev for electrons. These values were used to estimate the proton and electron energy flux on the lunar surface.

The soft UV flux from the solar corona requires further discussion. A light curve for the annular eclipse of the solar corona by the earth was calculated for an observer on the moon located at -35° selenographic longitude and +23° selenographic

latitude. A graphical integration of the eclipse was made for a circular corona consisting of eight rings with radii from 1.5 to 9.5 solar units. The brightness of each ring was based on the brightness distribution given by Van de Hulst [1953]. The value shown in Figures 3 is for the beginning of totality. It was assumed that the corona was a neutral scatterer, a good assumption in this spectral region. In the soft x-ray spectral region $\lambda < 100$A, not shown, the coronal spectrum is dominated by emission lines. Theoretical estimates indicate that the energy flux in this spectral region is low enough so that the soft x-ray photons from the annularly eclipsed corona can be neglected as a source of irradiation of the lunar surface [Widing, 1966].

The sources of irradiation permitted by geometry are shown on the left side of Figure 3. The lunar surface is shielded from the solar wind by the earth's magnetosphere. Resonance scattering of hard solar UV radiation by the geocorona is a process permitted by geometry but an estimated upper limit shows that this source of irradiation is negligible. The soft UV flux from the outer solar corona is comparable in magnitude with the observed integrated optical flux during totality. The medium and hard UV flux from the outer corona can be shown to be negligible.

The maximum intensities of luminescent photons, for an assumed luminescence efficienty of 10^{-3} typical of transparent solids, produced by the largest sources of irradiation are shown on the right side of Figure 3. They are 1% or less of the observed optical flux. The observed optical flux was integrated over the wavelength interval 0.33-0.55 μ. Visual observation suggest that the maximum intensity occurred at a larger wavelength. Thus the optical flux shown in Figure 3 is a lower limit. The luminescence efficiency is the ratio of input power to output power. Thus the luminescent intensities in Figure 3 are larger than the intensities of luminescent photons that are emitted outward within one optical depth of the lunar surface.

8. Conclusions

The 18 October 1967 total eclipse of the moon was a normal eclipse i.e. bright $A_{1.81} > 10^{-5}$ and red B - V $\tilde{-}$ 6. The moon at totality was nonuniformly illuminated, presumably due to variable cloud attenuation along the earth's terminator.

The possibility of direct excitation of lunar luminescence was examined by comparing the observed optical flux with the electron, proton and plasma fluxes measured by the lunar orbiting satellite Explorer 35 and with low energy proton and electron measurements by OGO III and Explorer 34. All known processes

of irradiation were considered and only two have sufficient magnitude to produce significant luminescent intensities. They are low energy electrons and protons and soft UV photons from the outer solar corona. The maximum percentage of direct luminescent photons is a fraction of 1% of the observed photon flux. This is calculated by assuming a typical luminescence efficiency of 10^{-3} for transparent materials.

The observations presented in this study confirm the conclusions of Ney, Woolf and Collins with regard to normal eclipses i.e. "There is relatively little energy available at the surface of the moon to cause luminescence." However the representative measurements of the energy density in the earth's tail are smaller than the values they used and the effective cosmic ray energy flux is much smaller than the value they used. It appears that soft UV photons from the outer corona can give a 2% contribution to the reflected soft UV flux from the moon.

Acknowledgements

M.J. Gaffey assisted in making the observations and in the data reduction. D.N. Bangston and R.S. Patterson also assisted with the data reduction and analysis. Mrs. L. Weinstein typed the manuscript and tables.

I am indebted to J.A. Van Allen, S.M. Krimigis, L.A. Frank and A.J.Lazarus for providing unpublished data and for a number of helpful discussions. I would like to thank Dr. Van Allen for critically reading the manuscript. This research was supported in part by the National Aeronautics and Space Administration under Grant NsGr 233-62.

REFERENCES

Frank, L.A., Preliminary data on low energy protons and electrons in the earth's tail, (personel communication), 1967.

Harris, D.L., Photometry and colorimetry of planets and satellites, in The Solar System 3, Planets and Satellites, edited by G.P. Kniper, pp. 272-342, University of Chicago Press, Chicago, Illinois, 1961.

Lazarus, A.J., Preliminary data for the plasma probe on Explorer 35, (personel communication), 1967.

Neff, J.S., Relative and absolute photometry of 185 stars, Astron. J., submitted for publication, 1967.

Neff, J.S., R.D. Carlson and R.R. Becker, The University of Iowa digital photometer, University of Iowa technical report 67-68, 1967.

Neff, J.S., and L.D. Travis, Properties of an intermediate band-pass photometric system, Astron. J., 72, 48-58, 1967.

Ney, E.P., N.J. Woolf, and R.J. Collins, Mechanisms for lunar luminescence, J. Geophys. Res., 70, 1787-1793, 1966.

Van Allen, J.A., Preliminary survey of the X-ray eclipse of the sun as viewed from Explorer 35 on 18 October 1967, University of Iowa Report 67-62 of 30 October 1967.

Van Allen, J.A., and S.M. Krimigis, Preliminary data on proton and electron measurements from Explorer 35, (personel communication), 1967.

Van de Hulst, H.C., The chromosphere and corona, in The Solar System 1, The Sun, edited by G.P. Kuiper, pp. 207-321, University of Chicago Press, Chicago, Illinois, 1953.

Widing, K.G., Interpretation of the soft X-ray spectrum of the sun, Astrophys. J., 145, 380-399, 1966.

667-1094

BLOCK DIAGRAM OF THE INTEGRATING DIGITAL PHOTOMETER
WITH SEMI AUTOMATIC PRINTING AND PUNCHING

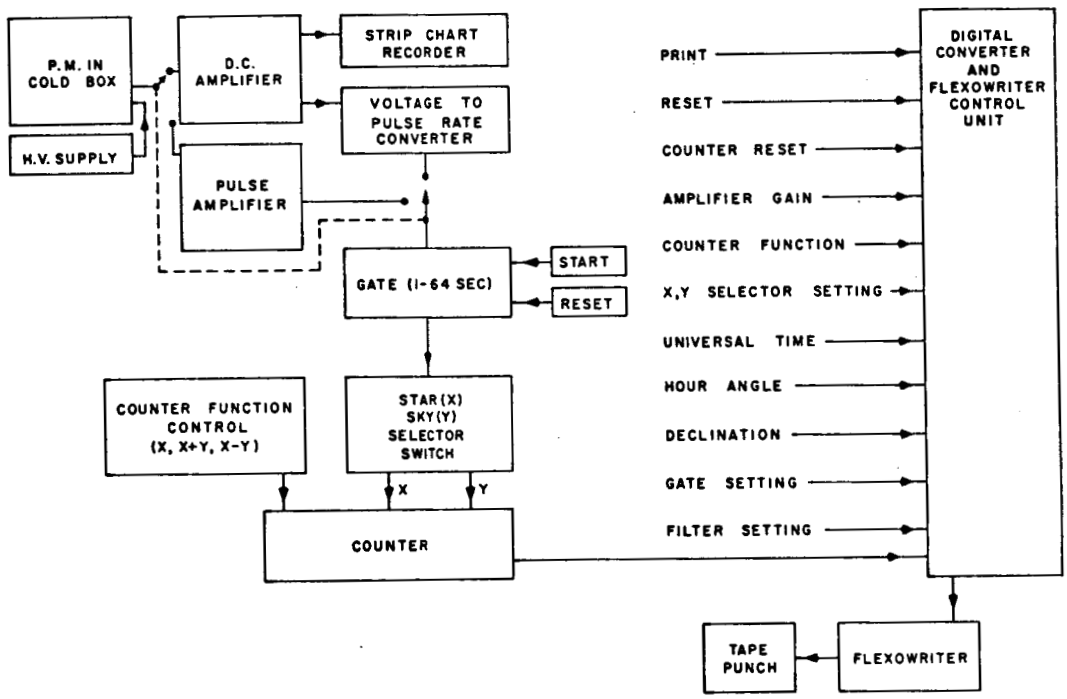

Fig.1.- The block diagram for the integrating digital photometer used in this study. The D.C. amplifier gain covers 6 decades and the amplifier output for the 36 possible ranges is converted into a 0-1kc/s frequency. This frequency is passed through a 1-64 sec gate to a reversing counter. Upon the command of the observer the following data is printed and punched on paper tape: the UT., the hour angle and declination of the telescope, the filter code, gain code and integration time, the counter function, channel and total. Additional information can be typed in by the observer.

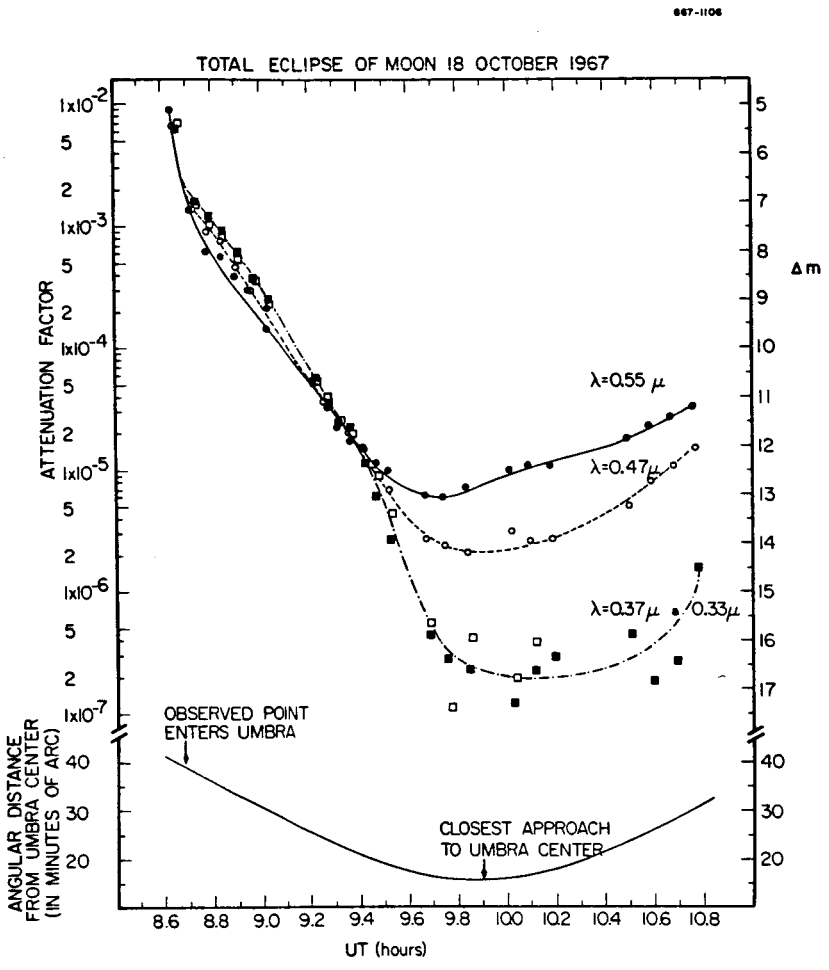

Fig. 2a.- The time variations of the monochromatic attenuation factors are shown. Note the remarkable similarity for all four curves for UT< $9^h.4$ and the abrupt decrease in A_σ for the two shortest wavelengths. Note also the asymmetry of the curves during total eclipse.

Fig. 2b.- The angular distance of the observed point on the moon from the umbra center is shown as a function of time.

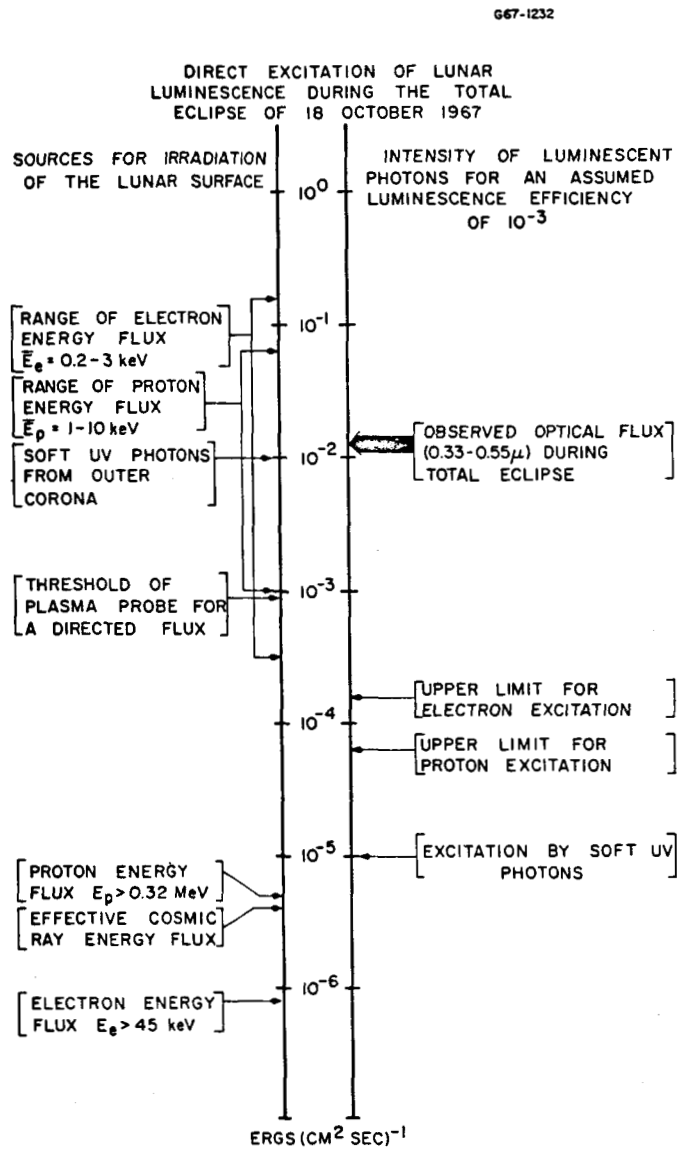

Fig. 3.- The sources of irradiation for the moon are shown on the left side of the figure. On the right side of the figure the observed optical flux emitted at the moon's surface is compared with the directly excited flux of luminescent photons.

Table I

Characteristics of the Detectors

$\lambda(\mu)$	0.550	0.470	0.370	0.330	λ of peak transmission
$\Delta\lambda$(in Å)	217	193	145	343	Equivalent rectangular bandpass
σ_o(in $10^4 cm^{-1}$)	1.818	2.129	2.702	2.949	Constant energy wavenumber
$\bar{E}_{h\nu}$(in ev)	2.254	2.639	3.350	3.656	Mean photon energy
$\Delta E_{h\nu}$(in ev)	0.068	0.082	0.155	0.291	rms width of detectors
$*F^o_{h\nu}$[photons $(cm^2 sec)^{-1}$]	1.69×10^5	1.95×10^5	1.27×10^5	1.60×10^5	Photon flux for a mean A0V star with $m_{0.55}=0.000$
$F_{h\nu}$[photons $(cm^2 sec)^{-1}$]	8.99×10^{15}	7.46×10^{15}	4.03×10^{15}	5.20×10^{15}	Solar photon flux at 1AU.

$*F_{h\nu} = F^o_{h\nu}(\sigma)\ 10^{-0.4 m_\sigma}$

Table II

Calculation of the Photon Flux Incident on the Surface of the Moon

Semi diameter of diaphragm	0'.352			
Semi diameter of moon	14'.713			
R = Distance to moon	4.06×10^5 km			
r = Radius of observed area on moon	41.6 km			
z = Zenith distance of sun at observed point on moon	40°30'			
$\frac{R^2}{r^2 \cos^2 z}$ = geometric factor	1.65×10^8			
$\varphi(\alpha)$ = phase factor =	1 since $\alpha \cong 0$			
$\lambda(\mu)$	0.550	0.470	0.370	0.330
P = geometric albedo	0.115	0.100	0.065	0.050
$\frac{R^2}{Pr^2 \cos^2 z} F_\sigma$ (at earth)	$1.43 \times 10^9 F_{1.81}$	$1.65 \times 10^9 F_{2.13}$	$2.54 \times 10^9 F_{2.70}$	$3.30 \times 10^9 F_{2.95}$

Table III

$\lambda = 0.550\ \mu$

UT (hours)	$F_{h\nu}$ (at earth) [photons$(cm^2 sec)^{-1}$]	Incident $F_{h\nu}$ (on moon) [photons$(cm^2 sec)^{-1}$]	Attenuation Factor
8.643	$5.54 \pm 0.11 \times 10^{4}$	7.92×10^{13}	8.81×10^{-3}
.710	$7.37 \pm .15 \times 10^{3}$	1.05	1.17
.774	$3.99 \pm .08$	5.70×10^{12}	6.35×10^{-4}
.835	$3.53 \pm .07$	5.05	5.62
.894	$2.49 \pm .05$	3.56	3.96
8.950	$1.85 \pm .04$	2.64	2.94
9.015	$9.26 \pm .28 \times 10^{2}$	1.32	1.47
.223	$2.13 \pm .06$	3.04×10^{11}	3.39×10^{-5}
.270	$1.67 \pm .05$	2.39	2.66
.315	$1.40 \pm .04$	2.00	2.23
9.365	$1.09 \pm .03$	1.56	1.73
.417	$9.65 \pm .29 \times 10^{1}$	1.38	1.53
.465	$7.14 \pm .28$	1.02	1.14
.519	$6.35 \pm .25$	9.08×10^{10}	1.01
.672	$4.02 \pm .16$	5.75	6.39×10^{-6}
9.742	$3.84 \pm .15$	5.49	6.11
.833	$4.50 \pm .17$	6.44	7.16
10.012	$6.46 \pm .26$	9.24	1.03×10^{-5}
.093	$6.73 \pm .27$	9.63	1.07
.179	$6.75 \pm .27$	9.65	1.07
10.488	$1.13 \pm .03 \times 10^{2}$	1.61×10^{11}	1.80
.578	$1.47 \pm .04$	2.10	2.34
.670	$1.72 \pm .05$	2.46	2.74
.759	$2.10 \pm .06$	3.00	3.34

Table III (continued)

$\lambda = 0.470\ \mu$

UT (hours)	$F_{h\nu}$ (at earth) [photons$(cm^2 sec)^{-1}$]	Incident $F_{h\nu}$ (on moon) [photons$(cm^2 sec)^{-1}$]	Attenuation Factor
8.650	$2.93 \pm 0.06 \times 10^{4}$	4.83×10^{13}	6.48×10^{-3}
.719	$6.22 \pm .12 \times 10^{3}$	1.03	1.38
.780	$4.00 \pm .08$	6.60×10^{12}	8.85×10^{-4}
.840	$3.42 \pm .07$	5.64	7.56
.901	$2.09 \pm .04$	3.45	4.62
8.957	$1.35 \pm .03$	2.22	2.98
9.023	$9.77 \pm .20$	1.61	2.16
.228	$2.41 \pm .05$	3.98	5.33
.274	$1.53 \pm .05$	2.53	3.39
.318	$1.09 \pm .03$	1.80	2.42
9.369	$8.69 \pm .26 \times 10^{1}$	1.43	1.92
.420	$6.96 \pm .21$	1.15	1.54
.468	$3.79 \pm .15$	6.25×10^{10}	8.38×10^{-6}
.523	$3.12 \pm .12$	5.15	6.90
.677	$1.22 \pm .05$	2.01	2.70
9.752	$1.10 \pm .04$	1.82	2.43
.843	$9.34 \pm .37 \times 10^{0}$	1.54	2.07
10.020	$1.43 \pm .06 \times 10^{1}$	2.35	3.15
.101	$1.19 \pm .05$	1.97	2.64
.187	$1.22 \pm .05$	2.01	2.70
10.500	$2.46 \pm .07$	4.06	5.44
.587	$3.70 \pm .11$	6.10	8.18
.680	$4.89 \pm .15$	8.08	1.08×10^{-5}
.769	$6.86 \pm .21$	1.13×10^{11}	1.52

Table III (continued)

$\lambda = 0.370\ \mu$

UT (hours)	$F_{h\nu}$ (at earth) [photons$(cm^2 sec)^{-1}$]	Incident $F_{h\nu}$ (on moon) [photons$(cm^2 sec)^{-1}$]	Attenuation Factor
8.661	$1.00 \pm .02 \times 10^{4}$	2.54×10^{13}	6.31×10^{-3}
.727	$2.52 \pm .05 \times 10^{3}$	6.40×10^{12}	1.59
.788	$1.93 \pm .04$	4.90	1.21
.849	$1.48 \pm .03$	3.75	9.33×10^{-4}
.907	$9.93 \pm .20 \times 10^{2}$	2.52	6.26
8.970	$6.01 \pm .12$	1.53	3.79
9.031	$4.02 \pm .08$	1.02	2.53
.233	$8.89 \pm .25 \times 10^{1}$	2.26×10^{11}	5.60×10^{-5}
.278	$5.83 \pm .18$	1.48	3.67
.323	$4.10 \pm .12$	1.04	2.58
9.373	$3.59 \pm .12$	9.13×10^{10}	2.26
.425	$1.80 \pm .06$	4.57	1.13
.473	$9.50 \pm .25 \times 10^{0}$	2.41	5.99×10^{-6}
.531	$4.26 \pm .30$	1.08	2.69
.686	$7.00 \pm .50 \times 10^{-1}$	1.78×10^{9}	4.41×10^{-7}
9.764	$4.38 \pm .35$	1.11	2.76
.853	$3.53 \pm .35$	8.97×10^{8}	2.23
10.033	$1.89 \pm .19$	4.81	1.19
.117	$3.49 \pm .35$	8.87	2.20
.199	$4.65 \pm .40$	1.18×10^{9}	2.93
.513	$7.11 \pm .50$	1.80	4.48
.599	$2.92 \pm .30$	7.42×10^{8}	1.84
.691	$6.76 \pm .50$	1.72×10^{9}	4.26
.781	$2.48 \pm .20 \times 10^{0}$	6.30	1.56×10^{-6}

Table III (concluded)

$\lambda = 0.330\ \mu$

UT (hours)	$F_{h\nu}$ (at earth) [photons$(cm^2 sec)^{-1}$]	Incident $F_{h\nu}$ (on moon) [photons$(cm^2 sec)^{-1}$]	Attenuation Factor
8.671	$1.11 \pm .02 \times 10^{4}$	3.65×10^{13}	7.04×10^{-3}
.735	$2.31 \pm .05 \times 10^{3}$	7.62×10^{12}	1.47
.797	$1.67 \pm .03$	5.51	1.06
.854	$1.29 \pm .02$	4.25	8.18×10^{-4}
.912	$8.24 \pm .16 \times 10^{2}$	2.72	5.23
8.978	$5.33 \pm .10$	1.76	3.38
9.036	$3.65 \pm .07$	1.21	2.32
.239	$8.38 \pm .25 \times 10^{1}$	2.76×10^{11}	5.32×10^{-5}
.283	$6.46 \pm .18$	2.13	4.10
.330	$4.19 \pm .12$	1.38	2.66
9.379	$3.17 \pm .12$	1.05	2.01
.431	$1.77 \pm .06$	5.83×10^{10}	1.12
.478	$1.41 \pm .06$	4.65	8.94×10^{-6}
.536	$5.24 \pm .30 \times 10^{0}$	1.73	3.32
.693	$8.59 \pm .50 \times 10^{-1}$	2.83×10^{9}	5.45×10^{-7}
9.775	$1.71 \pm .19$	5.65×10^{8}	1.09
.862	$6.53 \pm .50$	2.15×10^{9}	4.14
10.041	$3.03 \pm .30$	1.00×10^{9}	1.92
.124	$6.01 \pm .50$	1.98×10^{9}	3.81